Tailoring Wettability and Substrate Adherence of Thin Polymer Films with Surface-Segregating Bottlebrush Copolymer Additives

Journal:	*Langmuir*
Manuscript ID	la-2023-00703t.R1
Manuscript Type:	Article
Date Submitted by the Author:	26-Apr-2023
Complete List of Authors:	Laws, Travis; University of Tennessee, Chemical and Biomolecular Engineering Mei, Hao; Rice University, Terlier, Tanguy; Rice University, Shared Equipment Authority Verduzco, Rafael; Rice University, Chemical and Biomolecular Engineering Stein, Gila; University of Tennessee, Chemical and Biomolecular Engineering;

Tailoring Wettability and Substrate Adherence of Thin Polymer Films with Surface-Segregating Bottlebrush Copolymer Additives

Travis S. Laws,[y] Hao Mei,[z] Tanguy Terlier,[{] Rafael Verduzco,*[z,x] and Gila E. Stein*[y]

yDepartment of Chemical and Biomolecular Engineering, University of Tennessee, Knoxville, Tennessee 37996, USA

zDepartment of Chemical and Biomolecular Engineering, Rice University, Houston, TX 77005, USA

{SIMS Lab, Shared Equipment Authority, Rice University, Houston, TX 77005, USA

xMaterials Science and NanoEngineering, Rice University, Houston, TX 77005, USA

E-mail: rafaelv@rice.edu; gstein4@utk.edu

Abstract

We developed \reactive" bottlebrush polymers based on styrene (S) and tertbutyl acrylate (tBA) as additives for polystyrene (PS) coatings. The bottlebrush polymers spontaneously bloom to both the air and substrate interfaces during solution casting. While neat PS lms are hydrophobic and poorly adhere to the native oxide on clean silicon wafers, the hydrophilicity and substrate adherence of bottlebrush-incorporating PS lms can be tailored through the thermally-activated deprotection of tBA to produce acrylic acid (AA) and acrylic anhydride (AH). A critical design parameter is the manner by which tBA is incorporated

in the bottlebrush: When the bottlebrush side chains are copolymers of S and tBA, the extent of deprotection is extremely low, even after prolonged thermal annealing at elevated temperature. However, when the bottlebrush contains a mixture of poly(tertbutyl acrylate) (PtBA) and PS side chains, nearly all tBA is converted to AA and AH. Consequently, using the \mixed chain" bottlebrush design with thermal processing and appropriate conditioning, the water contact angle is reduced from over 90 on unmodied PS down to 75 on bottlebrush-incorporating PS lms, and the substrate adherence is improved in proportion to the extent of tBA deprotection.

Introduction

Many commodity polymers, such as PS, are hydrophobic with poor adherence to high-energy surfaces such as metal oxides.[1,2] It is possible to tailor the surface properties and substrate interactions of such materials by employing block copolymer surfactants,[3{5] adhesion-promoting layers,[6{8] or post-processing treatments,[9{11] but there are disadvantages to these methods: Block copolymer surfactants can form micelles that dissolve inside the bulk polymer[12] in addition to accumulating at the air surface and/or substrate. Adhesion-promoting layers are usually applied to the substrate prior to depositing the polymer,[13] which adds another step to the manufacturing process, and these layers may require a post-deposition treatment to activate the adhesion chemistry.[14] Post-deposition surface modication of the polymer, such as with plasma treatment, also adds another step to the manufacturing process and the functionality often degrades with time.[15]

Studies have shown that highly-branched polymer additives, such as many-armed star and bottlebrush architectures, can be designed to de-mix from the host polymer and segregate at lm interfaces during processing.[16,17] As an example, many-armed star or bottlebrush poly(styrene-r-methyl methacrylate) additives were shown to de-mix from a blend with linear poly(styrene-block-methyl methacrylate) and segregate at both the air and substrate

surfaces. The surface enrichment occurred during solution casting and persisted through thermal annealing. This process created a neutral topcoat that stabilized a perpendicular orientation of the self-assembled block copolymer domains relative to the surfaces,[18,19] making these additives useful for applications in lithography. In our own works, we established guidelines to design surface-active bottlebrush polymer additives for linear homopolymers. We considered systems with attractive,[20] neutral,[21] or repulsive[22] interactions between the bottlebrush and linear polymers, and measured the through-lm composition in both solution-cast and thermally-annealed lms. In all of these cases, the bottlebrush polymers and linear polymers had similar surface energies, and the bottlebrush additives were accumulated at both the free surface and substrate when the homopolymer chain length was much longer than the bottlebrush side chain length, consistent with an entropy-mediated segregation process.[16,23{25] As the interaction strength between bottlebrush and linear polymers changed from attractive to repulsive, the amount of bottlebrush additive at the lm interfaces was increased relative to the amount in the lm interior. Notably, in repulsive systems, nearly all of the bottlebrush additive was driven toward the lm boundaries.[22]

The present study is focused on the design of bottlebrush copolymer additives that tailor both the surface wettability and substrate adherence of commodity polymers. Linear PS was chosen as a model commodity polymer because it is hydrophobic and poorly adheres to oxide surfaces.[1,2] The bottlebrush copolymer additives were designed with both tBA and S moieties in the side chains, where tBA is a \functional" chemistry and S is incorporated to help compatibility with the linear PS host. We chose tBA as our functional chemistry for three reasons: First, tBA is a low energy, hydrophobic chemistry that is converted to AA (and subsequently AH) by heating at moderate temperature.[26] AA is a hydrophilic and pH-responsive chemistry.[26{28] As such, the incorporation of tBA provides a method to tune surface energy and wettability by simply heating the lm. Second, polymers with acrylate or carboxylic acid groups tend to stick to oxides due to hydrogen bonding.[1,2] Specically, the carbonyl group of tBA and AA is a hydrogen-bond acceptor, the carboxylic acid of AA is

a hydrogen-bond donor, and silicon oxide is both an acceptor and donor.[29,30] Consequently, both tBA and AA could improve adherence of the PS lm to an underlying oxide surface. More generally, AA comonomers are frequently employed to tailor adhesive properties of commodity polymers, both in air and in water.[31{35] Third, tBA/S enthalpic interactions are repulsive.[26,36] Consequently, nearly all bottlebrush additive should be localized at the surfaces after lm processing, provided the linear PS has a much higher molecular weight than the bottlebrush side chains.[21,22]

In the rst part of this manuscript, we describe the synthesis of these functional bottlebrush copolymer additives, examine the kinetics of tBA thermolysis, and characterize surface properties as a function of tBA conversion. Two types of bottlebrush copolymer additives were synthesized: those that contained a mixture of PtBA and PS side chains, designated as BB-(PtBA-m-PS), and those that contained P(tBA-r-S) side chains, designated as BB-P(tBA-r-S). We found that thermolysis kinetics at 140 C was signicantly accelerated in BB-(PtBA-m-PS) relative to BB-P(tBA-r-S), with conversions of approximately 95% versus 10-30%, respectively, after 48 hours of annealing. Consequently, thermal annealing could be used to tailor certain properties of BB-(PtBA-m-PS), such as surface wettability and substrate adherence, but had little impact on the properties of BB-P(tBA-r-S). In the second part of this manuscript, we examine the structure of PS lms that contain BB-(PtBA-m-PS) and BB-P(tBA-r-S) additives. For both cases, solution-cast lms showed a strong enrichment of the additive near the free surface with little additive remaining in the bulk. However, during a subsequent thermal annealing that activates tBA thermolysis, only BB-(PtBA-m-PS) remained localized at both the free surface and substrate interface. The nal part of this manuscript examines the properties of PS lms with BB-(PtBA-m-PS) additive, and shows that surface wettability and adherence to silicon surfaces (with native oxide) are both highly tunable and pH responsive.

Experimental

Materials

Linear Polystyrene.

A PS standard was purchased from Scientic Polymers, Inc.

Reagents.

Unless otherwise specied, all reagents and solvents were purchased from commercially available sources and used as received. Styrene and tert-butyl acrylate were passed through an aluminum oxide column before use. 2,2'-Azobis(2-methylpropionitrile) (AIBN) was puried by recrystallization in methanol. Bicyclo[2.2.1]hept-5-en-2-ylmethyl 2-(((dodecylsulfanyl)(thioxo)methyl)sulfanyl)-2-methylpropoanoate (NB-CTA)[37] and the third-generation Grubbs ($(H_2IMes)(\text{-}Pyr)_2(Cl)_2RuCHPh$) (G3) catalyst[38] were synthesized according to previously reported methods.

Norbornene functionalized poly(t-butyl acrylate) macromonomer (NB-PtBA).

t-Butyl acrylate (4492.1 mg, 35.0 mmol), NB-CTA (239.2 mg, 0.508 mmol), AIBN (8.6 mg, 0.052 mmol), and 2-butanone (4.9 mL) were added into a round-bottom ask equipped with a stir bar. The solution mixture was purged with argon for 20 min, and the polymerization was initiated by placing the ask in an oil bath at 60 C. After 1.5 h, the polymerization was quenched by immersing the ask into liquid nitrogen. The polymer was then obtained by precipitation into ice-cold methanol containing 40% H_2O (v/v). This purication was repeated four more times to ensure removal of all unreacted reagents.

Norbornene functionalized polystyrene macromonomer (NB-PS).

Styrene (10,389.9 mg, 99.90 mmol), NB-CTA (317.9 mg, 0.6752 mmol), AIBN (11.1

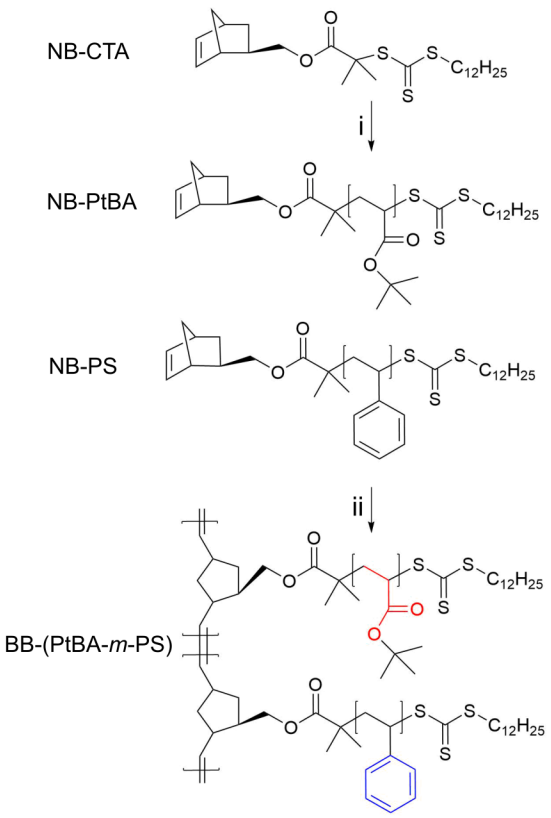

Scheme 1: (i) RAFT (t-butyl acrylate (2-butanone, 60 C), styrene (benzene, 70 C), AIBN); (ii) ROMP ($CHCl_3$, G3, RT). Fragments colored in red and blue were detected by TOF-SIMS analysis.

mg, 0.0678 mmol), and benzene (8.6 mL) were added into a 25 mL round-bottom ask equipped with a stir bar. The solution mixture was purged with argon for 20 min, and the polymerization was initiated by placing the ask in an oil bath at 70 C. After 18 h, the polymerization was quenched by immersing the ask into liquid nitrogen. The polymer was then obtained by precipitation into ice cold methanol. This purication was repeated four more times to ensure removal of all unreacted reagents.

Bottlebrush BB-(PtBA-m-PS) synthesis.

BB additives with a mixture of side chain chemistries were synthesized by ring-opening metathesis polymerization (ROMP) in a nitrogen lled glovebox. As shown in Scheme 1, NB-PtBA (118.4 mg, 0.0185 mmol, 55 equiv) and NB-PS (81.0 mg, 0.0150 mmol, 45 equiv)

were dissolved in anhydrous degassed chloroform (3.9 mL) in a vial equipped with a stir bar. In a separate vial a stock solution of G3 (2.44 mg/mL) was prepared in anhydrous degassed chloroform. Next, 0.1 mL (0.244 mg, 0.000335 mmol, 1 equiv.) of the catalyst solution was added to initiate the reaction and was allowed to stir for 30 min. The reaction was quenched by addition of a few drops of butyl vinyl ether and the product was collected by precipitation in cold methanol containing 10% H_2O (v/v).

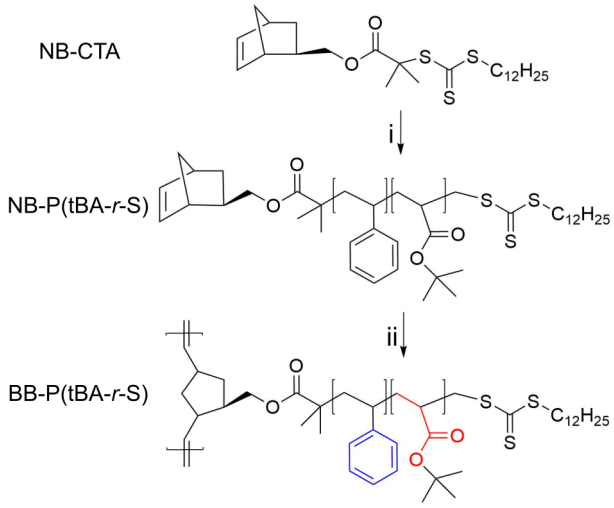

Scheme 2: (i) RAFT (70 C, t-butyl acrylate, styrene, AIBN, 2-butanone); (ii) ROMP ($CHCl_3$, G3). Fragments colored in red and blue were detected by TOF-SIMS analysis.

Norbornene functionalized poly(t-butyl acrylate-r-styrene) macromonomer (NB-P(tBA-r-S)).

NB-P(tBA-r-S) was synthesized by reversible addition-fragmentation chain-transfer (RAFT) polymerization. Styrene (3252.0 mg, 31.3 mmol), t-butyl acrylate (2632.0 mg, 20.5 mmol), NB-CTA (49.2 mg, 0.105 mmol), AIBN (3.9 mg, 0.024 mmol), and 2-butanone (3.5 mL) were added into a 25 mL round-bottom ask equipped with a stir bar. The solution mixture was purged with argon for 20 min, and the polymerization was initiated by placing the ask in an oil bath at 70 C. After 5 h, the polymerization was quenched by immersing the ask into liquid nitrogen. The polymer was then obtained by precipitation into ice cold

methanol containing 40% H_2O (v/v). This purication was repeated four more times to ensure removal of all unreacted reagents.

Bottlebrush BB-P(tBA-r-S) synthesis.

Random side-chain BB additives were synthesized in the same manner as the mixed side-chain BB. As shown in Scheme 2, NB-P(tBA-r-S) (76.4 mg, 0.0218 mmol, 150 equiv) was dissolved in anhydrous degassed tetrahydrofuran (0.63 mL) in a stir-bar equipped vial. A separate solution of G3 was prepared in anhydrous degassed tetrahydrofuran and 0.1 mL (0.106 mg, 0.000146 mmol, 1 equiv.) was added to initiate the reaction. After 30 min a few drops of butyl vinyl ether were added and the product collected by precipitation in cold methanol containing 10% H_2O (v/v).

ROMP kinetics.

ROMP kinetics were performed for certain NB-PtBA and NB-PS macromonomers. As a representative example, a NB-PtBA stock solution (59.4 mg/mL, DCM) was divided into nine vials equipped with stir bars (0.5 mL/vial, 29.71 mg polymer, 0.0046 mmol, 100 equiv). The solvent was removed under vacuum before placing the vials into the glovebox. One vial was kept as a reference (no G3 added) for NMR analysis. To the other 8 vials, anhydrous degassed chloroform (0.49 mL, 50 mg/mL) was added to dissolve the polymer followed by an injection of 0.1 mL (0.033 mg, 1 equiv) G3 solution to initiate each reaction. Each individual reaction was allowed to run for a predetermined time before being quenched by a few drops of butyl vinyl ether. The solvent was then removed under vacuum and 0.6 mL of $CDCl_3$ was added to each vial for NMR. Conversion was determined by comparison of the norbornene peaks (2H, 6.1 ppm) to the tert-butyl group (9H, 1.43 ppm) using the reference sample as a starting integration value. For styrene kinetics, integration was done against the styrene ring (5H, 6.3-7.2 ppm). GPC was then run to determine the degree of polymerization for each reaction time.

Instrumentation

Gel Permeation Chromatography (GPC)

Weight-average molecular weight (M_w) and dispersity (Đ) of each macromonomer and BB were determined at 25 C using an Agilent 1260 Innity II GPC with THF at a ow rate of 1.0 mL/min as the mobile phase. The Agilent GPC was equipped with a Wyatt Dawn Helios 8 multiangle light scattering detector, ViscoStar III, and an Optilab T-rEX. Reported molecular weights were obtained via conventional calibration analysis using polystyrene standards. GPC data are reported in Figure S1.

Nuclear Magnetic Resonance Spectroscopy (NMR)

^{1}H NMR spectra were measured on a 600 MHz Varian spectrometer. ^{1}H shifts are reported in ppm relative to internal solvents. Number-average molecular weight, M_n, was calculated by integration against the norbornene double bond protons (2H, 6.1 ppm). Example NMR spectra for PS, PtBA, and copolymer composition analysis are reported in Figures S2-S4.

Spectroscopic Ellipsometry

The thickness of each lm was measured using a J.A. Woollam M-2000 spectroscopic ellipsometer. The parameters that characterize the polarization change (phase change D and amplitude ratio Y) were recorded as a function of wavelength (l, nm), and these data were analyzed with a three-layer model of a Cauchy lm on native oxide/bulk silicon (ambient = air). The adjustable parameters for regression analysis were the constants A and B in the Cauchy dispersion relation, $n(l) = A + B/l^2$, as well as the lm thickness. Typical values of A and B were 1.5 and 0.01 cm^2, respectively. The refractive indexes for both the native oxide and bulk silicon were set to known values and the native oxide thickness was constrained to 1 nm.

Fourier-transfrom Infrared Spectroscopy (FTIR)

FTIR spectroscopy (Nicolet) was used to monitor the deprotection reaction of tBA to AA by tracking the absorbance of the C-O-C stretch at 1150 cm^{-1}.[39] The absorbances from styrene C-H between 3000-3100 cm^{-1} were used as reference peaks. The 1150 cm^{-1} peak areas (A_t) were normalized to the peak area at time t=0 (A_{t0}) before calculating the percent conversion of tBA to AA using the following equation.

$$\% \text{ conversion} = \frac{A_{t0} \quad A_t}{A_{t0}} \tag{1}$$

Time-of-Flight Secondary Ion Mass Spectrometry (TOF-SIMS)

TOF-SIMS depth prole analysis was conducted with an ION-TOF TOFSIMS V instrument (ION-TOF GmbH, Munster, Germany), administered by the Rice University Shared Equipment Authority. Measurements were performed using a Bi/Mn liquid metal primary ion gun (LMIG) and an argon gas cluster ion gun that were operated in non-interlaced, dual beam mode with alternating sputtering and analysis cycles. For all samples, the Ar_n^+ (10 keV, n = 1500) beam was rastered over a 500 mm^2 area with a central Bi_3^{2+} (30 keV) analysis region of 90 mm^2. An electron ood gun was used for charge compensation, operating at 20 eV with a lament current of 2.40 A and surface potential of 6.9 V. Negative secondary ions were collected at a rate of 2 frames/sec with a cycle time of 200 ms.

Flow Coating

The linear PS and BB copolymer, at a 9:1 ratio (w/w), were dissolved in chlorobenzene to produce a solids concentration of 5 wt %. Films were prepared by ow coating the blend solutions onto freshly UV-Ozone cleaned silicon wafers. UV-Ozone cleaning produces a thin oxide layer, and its presence was conrmed by contact angle goniometry (complete

spreading of a water droplet). The blade gap height was set to 500 mm and 50 mL of solution was injected into the gap. The coating speed was set to produce lms with a thickness of 350 50 nm. Thermal annealing at 140 C was performed in a nitrogen-lled glovebox.

Microscopy

Optical microscopy images were acquired with a Nikon LV100 reected light microscope at magnications of 2.5x, 20x, and 100x. Atomic force microscopy (AFM) was performed using an Asylum MFP-3D system in tapping mode. The probes were silicon with a spring constant of 9 N/m and resonance frequency of 115 kHz. Imaging parameters were 1 Hz scan frequency, 5 mm x 5 mm scan size, and 256 x 256 resolution. Raw height and phase images were processed using a rst-order attening, provided in the Asylum software, which helps eliminate z-osets between scan lines by subtracting an average z value (z = height or phase).

Contact Angle Goniometry

Static contact angle measurements were made using a DataPhysics OCA 15EC goniometer with DI water as the probe liquid. The contact angle measurements were recorded for 60 s at 9 frames/s from three dierent areas of the sample. The measurements were then plotted out against a logarithmic time scale, and the equilibrium angle was determined from the observed plateau.

Results and Discussion

Bottlebrush copolymer additives were synthesized using either a random copolymer NB-P(tBA-r-S) macromonomer or a mixture of NB-PS and NB-PtBA macromonomers. Bottlebrush copolymers based on NB-P(tBA-r-S) macromonomers are designated BB-P(tBA-r-S), while those based on a mixture of NB-PS and NB-PtBA macromonomers are designated BB-(PS-m-PtBA). The characteristics of the linear PS, the macromonomers, and the bot-

Table 1: Characteristics of the PS standard, macromonomers, and bottlebrush polymers. M_n is number-average molecular weight, N is degree of polymerization, Đ is dispersity, r is % conversion of macromonomer to bottlebrush, f_{tBA} is mol % of tBA in the monomer feed, and F_{tBA} is mol % of tBA in the nal polymer.

Polymer	M_n (kg/mol)	N[i]	Đ[i]	r	f_{tBA}	F_{tBA}
PS	58	558	1.07	-	0%	0%
NB-P(tBA-r-S)	3.0	26	1.2	-	40%	41%
NB-PtBA_1	4.3	34	1.1	-	100%	100%
NB-PS_1	4.5	43	1.1	-	0%	0%
NB-PtBA_2	6.4	50	1.1	-	100%	100%
NB-PS_2	5.4	52	1.1	-	0%	0%
BB-P(tBA-r-S)	156	74	1.3	100%	41%	41%
BB-(PtBA-m-$PS)_1$	353	80	1.4	85%	47%	43%
BB-(PtBA-m-$PS)_2$	476	80	1.3	92%	47%	47%

[i]For the bottlebrush polymers, N and Đ correspond to backbone lengths and dispersities, respectively.

tlebrush copolymers are listed in Table 1. The subscripts on polymer names indicate which macromonomers were used to synthesize each bottlebrush copolymers. For example, BB-(PtBA-m-$PS)_1$ was synthesized from NB-PtBA_1 and NB-PS_1. All macromonomers in Table 1 were synthesized through reversible addition-fragmentation chain-transfer (RAFT) polymerization using an exo-NB functionalized chain-transfer agent (CTA). The NB-P(tBA-r-S) macromonomer was synthesized by a reaction run at low conversion, which favors a statistical incorporation of each monomer,[40] and all other macromonomers were synthesized at high conversion. All bottlebrush copolymers were synthesized through ring-opening metathesis polymerization (ROMP) using a third generation Grubbs catalyst (G3).[37,41]

When synthesizing bottlebrush copolymers with \mixed" side chains, random incorporation is anticipated when the polymerization kinetics of each macromonomer are matched.[41] Otherwise, the bottlebrush copolymer could have a gradient in composition along its length, or even distinct blocks of each chemistry. Therefore, the ROMP homopolymerization kinetics were measured for NB-PtBA_2 and NB-PS_2. As seen in Figure 1, the homopolymerization of NB-PS_2 is approximately 2 times faster than that of NB-PtBA_2. This is opposite of the trend reported by others,[41] although a dierent norbornene was used in that study. Small angle x-ray scattering (SAXS) was performed on as-cast and annealed (140 C, 48 hrs) lms

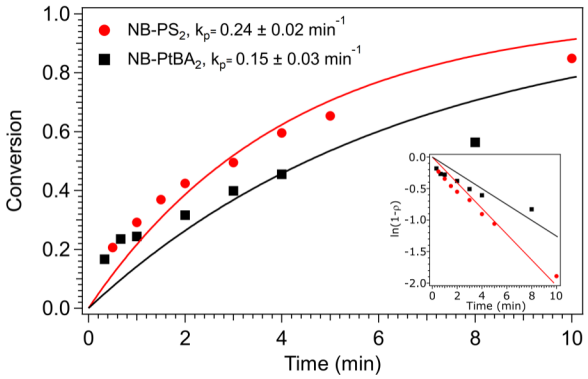

Figure 1: Analysis of ROMP kinetics for NB-PS_2 and NB-$PtBA_2$ homopolymerizations. Solid lines represent the t to $= 1 - e^{-k_p t}$. The k_p for each macromonomer is reported with an uncertainty of one standard deviation.

of BB-(PtBA-m-PS)$_1$ to check for self-assembly. If the side-chain incorporation is closer to blocky than random, then self-assembly could occur with a domain periodicity set by the backbone length. For an average backbone DP of 80, the anticipated domain periodicity of a blocky structure is on the order of 40 nm.[42] As seen in Figure S5, one broad peak is present at q = 0:6 nm, corresponding with a length scale of 10.5 nm. This is suggestive of a correlation between backbones due to side chain organization rather than blockiness along the backbone.

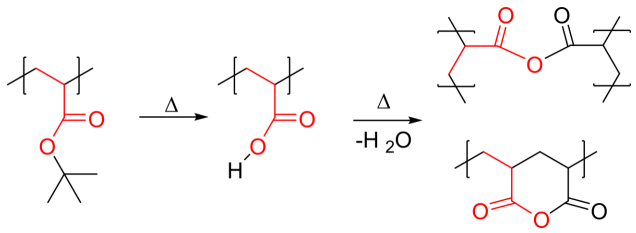

Scheme 3: Thermal deprotection of tBA to AA. A secondary reaction can occur where two AA units react and dehydrate to form AH crosslinks. Molecular fragments detected in TOF-SIMS are red.

A useful attribute of tBA-based additives is that heating at moderate temperature will activate a deprotection reaction that cleaves the tert-butyl ester to produce an AA moiety, as shown in Scheme 3.[43] Two AA moieties can then react to form AH, generating both intra- and inter-molecular linkages.[44] In the presence of water, AH will hydrolyze to revert to AA.[45,46] Two types of tBA-incorporating bottlebrush additives were synthesized (\random"

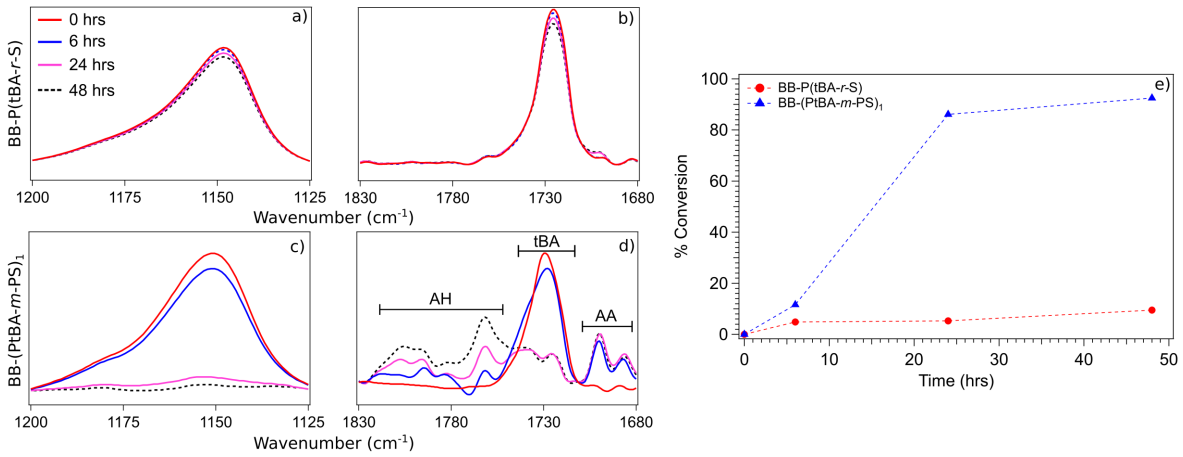

Figure 2: FTIR data showing the characteristic absorbances from C-O-C at 1150 cm^{-1} and C=O between 1830-1680 cm^{-1} for a,b) BB-P(tBA-r-S) and c,d) BB-$(PtBA\text{-}m\text{-}PS)_1$ lms as a function of annealing time at 140 C. e) Percent conversion of tBA to AA as a function of time for BB-P(tBA-r-S) and BB-$(PtBA\text{-}m\text{-}PS)_1$, calculated from the absorbance at 1150 cm^{-1}.

versus \mixed" side chains), and we rst examined the kinetics of thermal deprotection to test for any dierences between these designs. Films were annealed at 140 C for a total of 48 hrs, and FTIR data were acquired after 0, 6, 24, and 48 hrs. Figure 2 shows time-lapse FTIR data and percent conversion for two representative materials, BB-P(tBA-r-S) and BB-$(PtBA\text{-}m\text{-}PS)_1$, and Figure S6 shows percent conversion for a few additional materials. The deprotection reaction was monitored through changes in the C-O-C stretch at wavenumber 1150 cm^{-1}, and this absorbance was only slightly reduced for BB-P(tBA-r-S) yet was nearly undetectable for BB-$(PtBA\text{-}m\text{-}PS)_1$ after 48 hours (Figures 2a and 2c). The percent conversion of tBA is reported in Figure 2e and reached only 10% for BB-P(tBA-r-S) and exceeded 95% for BB-$(PtBA\text{-}m\text{-}PS)_1$ after 48 hours.

The secondary reaction that produces AH was monitored through changes in the C=O stretch, which is detected at wavenumbers in the range of 1750 to 1830 cm^{-1}. As seen in Figures 2b and 2d, the spectra for BB-P(tBA-r-S) show a strong signal at 1730 cm^{-1} that undergoes only a slight reduction with time. However, the spectra for BB-$(PtBA\text{-}m\text{-}PS)_1$ show a reduction in the absorbance at 1730 cm^{-1} with emergence of new peaks at both higher and lower wavenumbers. These changes are consistent with the loss of tert-butyl protecting

groups and formation of AA and AH moieties.[44,47,48] To test whether the formation of AH creates inter-molecular crosslinks, the solubility of BB-(PtBA-m-PS)$_1$ films was examined both before and after annealing at 140 C for 48 hrs. Films were immersed in tetrahydrofuran at room temperature, which is capable of dissolving all chemistries. While the as-prepared films were completely dissolved within a minute, the annealed films (> 95% conversion) did not dissolve after 5 min, consistent with the formation of a network-like structure due inter-molecular crosslinking.

The FTIR data and related analyses in Figures 2 and S6 clearly show that the rate of thermal deprotection depends on how tBA monomers are incorporated within the bottlebrush additive. We speculate that this stems from the auto-accelerated effect of nearby acidic protons on the deprotection kinetics, as is documented for the thermal deprotection of poly(p-t-butoxycarbonyloxystyrene) and poly(t-butylmethacrylate).[43,49,50] An auto-accelerated effect would be sensitive to the local concentration of both tBA and AA groups. In materials such as BB-P(tBA-r-S), the local concentration of these moieties is diluted by the presence of S comonomer. However, in materials such as BB-(PtBA-m-PS)$_1$, the PS and PtBA side chains could segregate into chemically-distinct domains along the bottlebrush backbone, thereby producing regions with an elevated local concentration of reactive moieties. Such segregation is consistent with the previously-discussed SAXS data.

As thermal annealing drives different extents of deprotection in the two types of bottlebrush copolymers, the surface wettabilities of annealed films are expected to differ. Water contact angles were measured on as-cast films, films that were thermally annealed at 140 C for 48 hrs, and films that were thermally annealed at 140 C for 48 hrs and then conditioned by soaking in either deionized water (pH ' 6) or 1N NaOH solution (pH ' 14) for 30 min. Figure 3 reports the outcomes for BB-P(tBA-r-S) and BB-(PtBA-m-PS)$_1$. As a reference, the water contact angles on linear PtBA, PS, and PAA surfaces were measured to be 88, 90, and 20, respectively. It is important to note that the water contact angle on PAA varies with the degree of H^+ dissociation, with values ranging from 70 (protonated) to 10

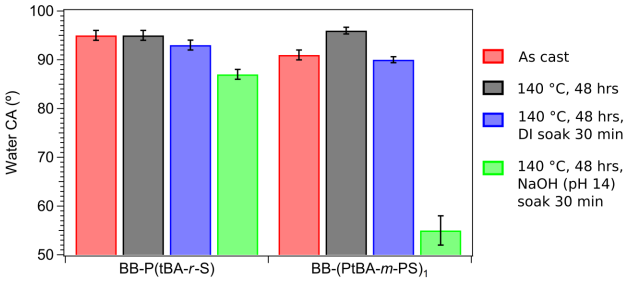

Figure 3: Water contact angle measurement data for BB-P(tBA-r-S) and BB-(PtBA-m-PS)$_1$ bottlebrush lms.

(deprotonated).[51] The extent of dissociation is controlled by the pK_a of the PAA, which has been reported to be approximately 8 for similar PAA polymer surfaces,[34,52{54] and by the pH of water, which is approximately 5-6 for deionized water (containing dissolved carbonic acid).

As-cast lms of BB-P(tBA-r-S) and BB-(PtBA-m-PS)$_1$ had water contact angles of 95 and 91, respectively, consistent with the hydrophobic nature of S and tBA moieties. After annealing, the water contact angle remained at 95 on BB-P(tBA-r-S) but increased to 96 on BB-(PtBA-m-PS)$_1$. After annealing and conditioning in deionized water, the water contact angle was 93 on BB-P(tBA-r-S) and 90 on BB-(PtBA-m-PS)$_1$. Finally, after annealing and conditioning in 1N NaOH solution, the water contact angles decreased to 87 on BB-P(tBA-r-S) and 55 on BB-(PtBA-m-PS)$_1$. These data show that the surface wettability of BB-(PtBA-m-PS)$_1$ is highly tunable through a combination of annealing and conditioning, while that of BB-P(tBA-r-S) is far less sensitive to the same treatments. Focusing on trends with BB-(PtBA-m-PS)$_1$ we note that the increase in hydrophobicity after annealing might be attributed to the presence of AH in addition to AA and S moieties, as AH is not hydrophilic.[55] Another point to consider is that side chains on BB-(PtBA-m-PS)$_1$ can rearrange during annealing. The surface energies of PS, PtBA, and PAA are 40.7 mJ/m^2,[56] 30.4 mJ/m^2,[57] and in the range of 35-60 mJ/m^2,[28,58,59] respectively, at 25C. During casting, PtBA is enthalpically preferred over PS at the free surface. This surface preference may change as tBA groups are converted to AA and AH, although it is hard to state denitively

which component in the blend has the lowest surface energy. This challenge is associated with the ill-dened chemistry of the bottlebrush additive (diering proportions of AH and AA, AH-AH crosslinking) as well as diculties in characterizing the surface energies of polyelectrolytes like PAA. However, soaking in DI will swell and expose AA-rich segments, accounting for the slightly lower contact angle after conditioning. Soaking in aqueous NaOH both swells and deprotonates AA-rich segments (NaOH pH > PAA pK_a)[34] to form the sodium salt, which produces the greater hydrophilic change when compared to the DI soak. Furthermore, strong bases like NaOH have been shown to enhance the rate of anhydride hydrolysis in copolymers of styrene and maleic anhydride.[45]

Our next goal was to demonstrate that these bottlebrush copolymers could serve as surface-active additives for linear PS, a commodity polymer, and tune both the surface hydrophilicity and adherence to a silicon substrate. When blended with linear PS, the bottlebrush copolymers should spontaneously segregate to the interfaces of a thin lm. This is due to a few factors: First, the surface energy of PtBA (30.4 mJ/m^2) is lower than that of PS (40.7 mJ/m^2), so PtBA is preferred over PS at the air-polymer interface. PtBA is also preferred over PS at the silicon substrate due to its capability to form hydrogen bonds with the native oxide.[29,30] Second, highly-branched polymers are entropically preferred over linear polymers at surfaces.[60] Third, the positive Flory-Huggins interaction parameter between PtBA and PS ($q_{PS\text{-}PtBA}$ ' 0.1)[61] favors de-mixing of the additive and linear host.[22,62] Additionally, the short bottlebrush copolymer side chains are poorly wet by the long PS chains, also favoring de-mixing.[21] However, deprotection of tBA to produce AA and AH will change the surface energy of the bottlebrush additive as well as its interactions with linear PS. This may disrupt enrichment of the additive at the free surface, either by promoting lateral phase separation or by driving diusion of additive into the interior of the lm.

The enrichment of bottlebrush copolymer additives at the free surface and substrate was examined through TOF-SIMS depth proling,[60] as shown in Figure 4. Thin lms of linear PS containing 10 wt% of either BB-P(tBA-r-S) or BB-(PtBA-m-$PS)_1$ additive were cast

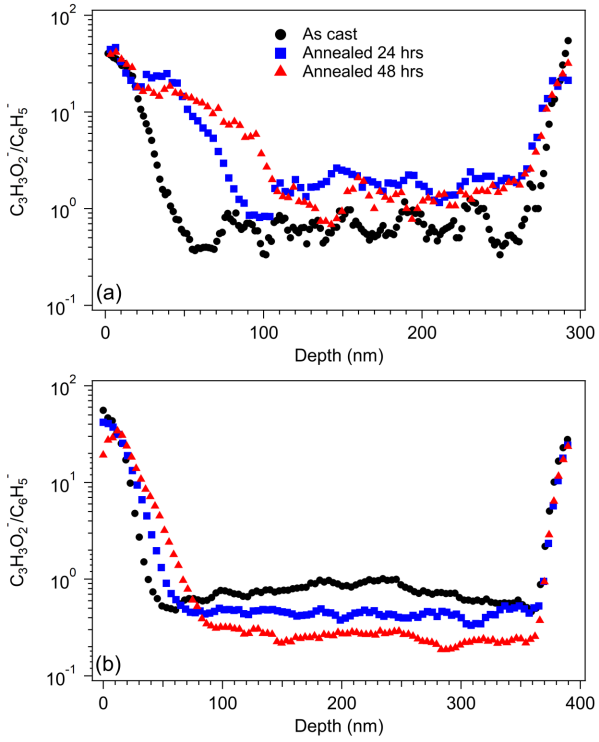

Figure 4: TOF-SIMS depth proles for thin lms of of linear PS with (a) BB-P(tBA-r-S) and (b) BB-(PtBA-m-PS)$_1$ additives. The ratio of $C_3H_3O_2^-$ to $C_6H_5^-$ signals is proportional to additive concentration. The polymer-air interface is at depth = 0 nm and the polymer-substrate interface is at depth = 300-400 nm (last signal point).

onto silicon substrates and measured without further processing (as cast), after annealing at 140 C for 24 hours, and after annealing at 140 C for 48 hours. The molecular fragments that are unique to S and tBA/AA/AH moieties are indicated by the blue ($C_6H_5^-$) and red ($C_3H_3O_2^-$) colors, respectively, in Schemes 1-3. In as-cast lms with either additive, the relative signal of $C_3H_3O_2^-/C_6H_5^-$ is strongly peaked at both ends of the depth prole, a clear indication of additive segregation at both surfaces. This outcome is consistent with our prior studies that examined surface segregation in blends having unfavorable bulk interactions between the bottlebrush copolymer and linear polymer, where the bottlebrush copolymer was also enthalpically preferred at both surfaces.[22,62] Thermal annealing had little impact on the segregation behavior of BB-(PtBA-m-PS)$_1$ but seemed to drive BB-P(tBA-r-S) away from the free surface and into the interior of the lm. These dierent behaviors in annealed samples are attributable to the dierences in chemistry: First, as previously discussed, the high tBA

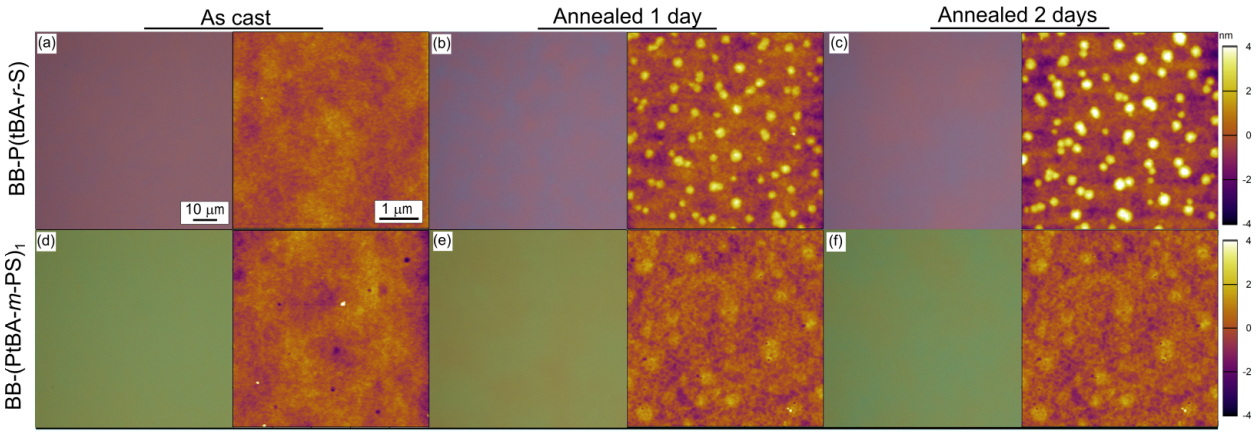

Figure 5: Optical and AFM images of PS lms with (a,b,c) BB-P(tBA-r-S) or (d,e,f) BB-(PtBA-m-PS)$_1$ additive as a function of annealing time at 140 C. Optical images are at 100X magnication and AFM height images are 5 mm x 5 mm.

conversion in BB-(PtBA-m-PS)$_1$ produces intermolecular crosslinks that could stabilize the bottlebrush-rich layers at each surface. Second, conversion of tBA to AA increases the Flory interaction parameter between the bottlebrush additive and linear PS ($q_{S\text{-}tBA}$ ' 0.1[61] vs $q_{S\text{-}AA}$ ' 0.9[63]), which creates a large energetic barrier opposing interdiusion.[61] This barrier is expected to be higher for BB-(PtBA-m-PS)$_1$ (95% nal conversion) than BB-P(tBA-r-S) (nal 10% conversion). The TOF-SIMS data in Figure 4 lend support to this point, as the bulk concentration of BB-P(tBA-r-S) is increased with annealing (depth of ca. 100 - 200 nm), while the bulk concentration of BB-(PtBA-m-PS)$_1$ is reduced with annealing. The dierent monomer sequences within each design, meaning the random copolymer side chains in BB-P(tBA-r-S) versus the mixture of dierent side-chain types in BB-(PtBA-m-PS)$_1$ could also impact their miscibility with linear PS.

Microscopy was used to examine the surface structure of the PS/additive blend lms. Figure 5 shows optical microscopy and atomic force microscopy (AFM) images for PS lms containing 10 wt% of either BB-P(tBA-r-S) or BB-(PtBA-m-PS)$_1$ additive as a function of annealing time. After casting, both types of surfaces were at and featureless. After annealing, lms with BB-P(tBA-r-S) additives developed roughness at a lateral scale of approximately 10 m, as evidenced by color variation in optical microscopy. Additionally,

small bumps with a height of 3-4 nm and diameter of 100-200 nm were detected by AFM. It is unclear whether these bumps are a sign of lateral phase separation between the bottlebrush and linear PS. In contrast, lms with BB-(PtBA-m-PS)$_1$ additive remained at through thermal annealing, although a subtle texture was observed by AFM. This dierence in surface features is most likely due to a combination of two factors: First, the mixed side chains in BB-(PtBA-m-PS)$_1$ could act as a compatibilizer for the linear PS due to their ability to rearrange around the bottlebrush backbone, suppressing the drive to restructure. Second, the crosslinking in BB-(PtBA-m-PS)$_1$ might help to lock-in the as-cast structure.

The bottlebrush copolymers with a mixture of PtBA and PS chains are more tunable than those with P(tBA-r-S) side chains, as evidenced by the thermolysis kinetics (Figure 2) and measurements of surface wettability (Figure 3). Furthermore, the thin lm blends of PS and mixed-chain bottlebrush copolymer undergo little restructuring with prolonged thermal annealing (Figure 4). With these factors in mind, the remainder of this study was focused on the functions aorded by BB-(PtBA-m-PS)$_1$ additive in PS. Thin lm blends of PS and 10 wt% BB-(PtBA-m-PS)$_1$ were annealed for dierent amounts of time at 140 C. PS lms without any additives were ow coated onto clean silicon and used as a control without further processing. The adherence of the lms to silicon substrates was examined by submersion in aqueous solutions of various pH for 30 min, after which the samples were rinsed with DI water and then dried under a nitrogen stream.

Figure 6 shows optical microscopy images of the samples before and after submersion tests. Pure PS lms (no additive) oated o the silicon substrate when soaked in DI, 1M NaCl, or 1M NaOH, as shown in Figure 6b-d. However, the adherence of additive-containing lms to silicon was a function of both annealing time (tBA conversion) and pH of the aqueous solution. As shown in Figure 6f-h, the as-cast lms (0% tBA conversion) remained adhered when submerged in DI water but released when submerged in 1M NaCl and 1N NaOH. We also observed that submersion in 1M NaCl produced a clean release, meaning an intact lm oated o the surface, while submersion in 1N NaOH produced a fractured release with

some residue left on the substrate. As shown in Figure 6j-l, lms that were annealed for 6 hours (15% tBA conversion) remained adhered when submerged in either DI and 1M NaCl and showed a fractured release after submersion in 1N NaOH. Annealing for 24 and 48 hrs (90-95% tBA conversion) results lms that remain adhered when submerged in all uids, as shown in Figure 6n-p and 6r-t.

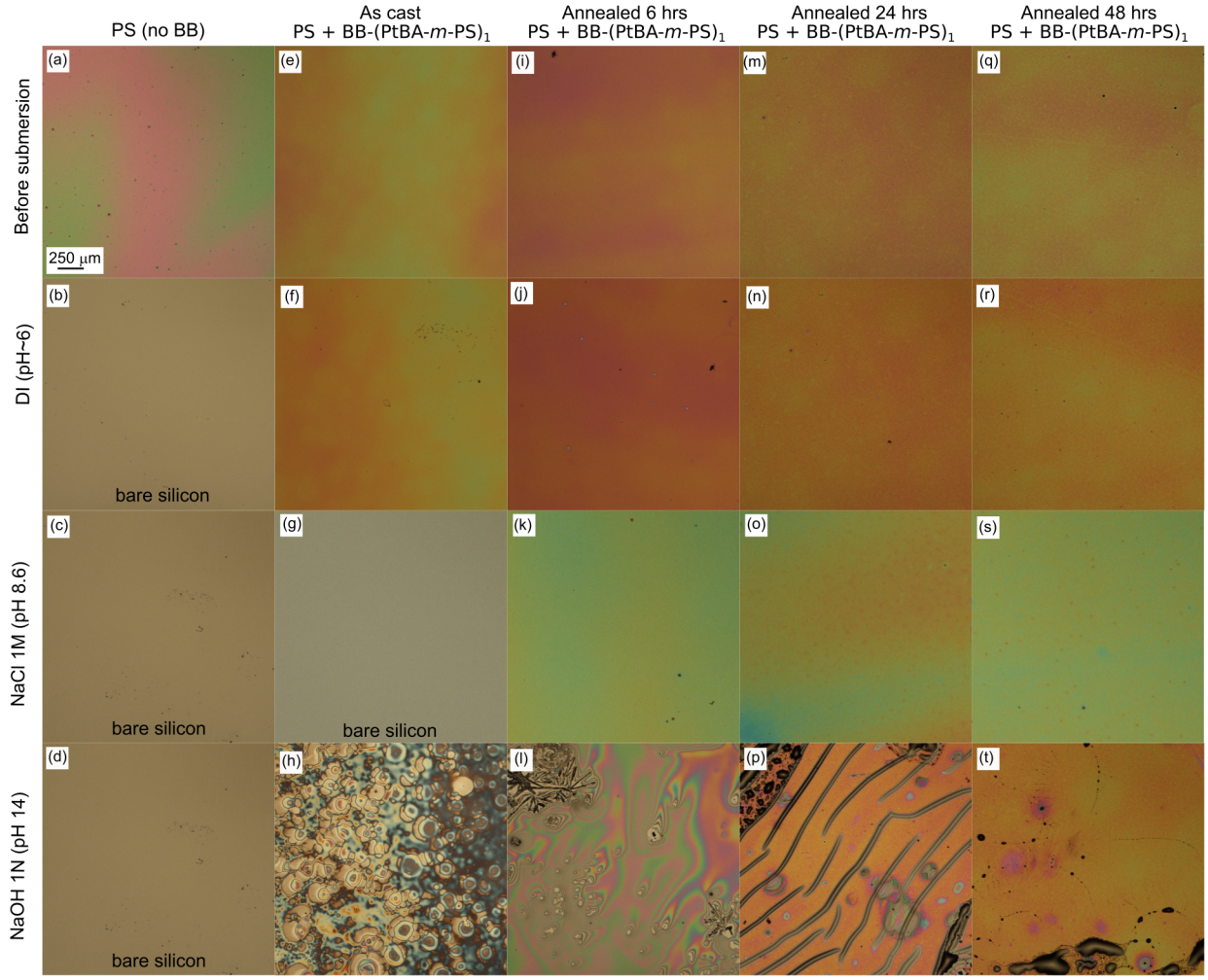

Figure 6: Optical images of PS and PS + BB-(PtBA-m-PS)$_1$ blend lms before and after submersion in DI, 1M NaCl, or 1N NaOH, where each row corresponds to a dierent treatment method. a-d) PS (no BB). e-h) As cast BB-(PtBA-m-PS)$_1$ blend. i-l) Annealed 6 hrs BB-(PtBA-m-PS)$_1$ blend. m-p) Annealed 24 hrs BB-(PtBA-m-PS)$_1$ blend. q-t) Annealed 48 hrs BB-(PtBA-m-PS)$_1$ blend. Annealing was done at 140 C.

AA groups are both a hydrogen-bond donor and acceptor, compared to tBA groups being only a hydrogen-bond acceptor, so the conversion of tBA to AA introduces additional

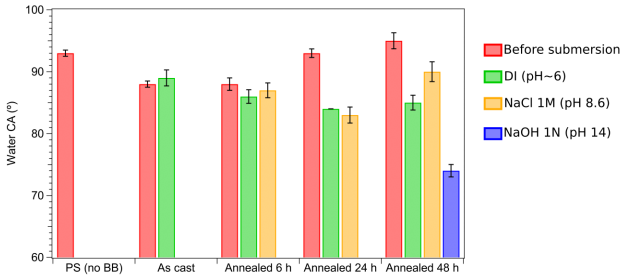

Figure 7: Water contact angle for each lm presented in Figure 6. Data are reported for lms that remain adhered to the surface through each treatment.

hydrogen-bonding sites between the additives and the substrate. All lms remain adhered in DI water due to two reasons: First, the ionic strength of DI water is negligible so it is not capable of disrupting these hydrogen bonds. Second, with additives containing PAA segments (6, 24, 48 h), the acid groups remain protonated due to the pK_a of the hydronium ion (H_3O^+, -1.74) being much lower than the pK_a of PAA (approximately 8[34,52{54]). This results in PAA retaining both its hydrogen-bonding donor and acceptor sites. When placed into a NaCl solution, only the lms containing PAA (6, 24, 48 h) remain adhered, indicating that the increased density of hydrogen-bonding sites provided by AA is necessary to protect the lm from release. Finally, when placed into an NaOH solution, lms remain adhered only when the additives contain a high amount of AA and AH moieties. The increased amount of AH is likely the major factor as to why the 24 and 48 h annealed lms remain intact in NaOH solution: anhydride groups are well-known adhesion promoters, such as in maleated poly(styrene-b-ethylene/butylene-b-styrene),[64] and intermolecular crosslinking will help to stabilize the lms. We note that some creasing was observed for lms that were annealed for 24 hr (Figure 6p), but not for lms that were annealed for 48 hr (Figure 6t), which underscores the role of AH moieties in this adherence process.

The trends in surface wettability that were observed with pure BB-(PtBA-m-PS)$_1$ lms are also observed when BB-(PtBA-m-PS)$_1$ is incorporated in PS. Figure 7 summarizes water contact angles for the blend lms as a function of annealing time at 140 C and the conditioning treatment. PS lms (no additive) were again used as a control. Contact angles

were only recorded for lms that remained adhered to the substrate through conditioning. Before submersion in any of the conditioning uids, all lms (as cast and annealed) had contact angles near or above 90. After annealing for 6 hrs and conditioning for 30 min in DI or 1M NaCl, the contact angles were all in the range of 87 - 90. Annealing for 24 hrs followed by the same conditioning protocols was found to slightly increase the hydrophilicity, producing contact angles near 85. Annealing for 48 hours followed by the same conditioning protocols produced a more varied response, where lms that were conditioned at lower pH (pH in the range of 6 to 9) produced water contact angles in the range of 85 to 90, while those conditioned at higher pH (pH of 14) produced water contact angles in the range of 75. These trends are similar to the ones seen in bottlebrush only lms, where the overall surface response to water is controlled by the dissociation of H^+ from AA along with the hydrolysis of AH to form AA.

Conclusions

We report the synthesis of two types of bottlebrush polymer additives for PS lms, both of which contain a mixture of S and \reactive" tBA units. The rst type of bottlebrush had copolymer side chains of S and tBA, while the second type had a mixture of PS and PtBA side chains. While both types of bottlebrush polymer additive bloomed to the surfaces of a PS lm during casting, only the \mixed chain" design remained strongly localized at the free surface (i.e., the interface with air) through a subsequent thermal annealing step. This eect is postulated to arise from inter-molecular AH crosslinks, a large energetic barrier to interdiusion of bottlebrush and PS, or a combination of both eects. Additionally, only the \mixed chain" design could be thermally deprotected to AA/AH with high conversion, which is attributed to an auto-catalytic eect associated with the high local concentration of reactive tBA moieties. Consequently, the \mixed chain" design leads to tunable surface properties, such as hydrophilicity and substrate adherence, through changes in both

deprotection level and pH.

The use of tBA as a reactive unit leads to other possibilities for future studies. The tertbutyl moiety is an acid labile protecting group, so if the formula were to include a photoacid generator (PAG), then the deprotection reaction could be spatially controlled by exposure to a pattern of UV light.[65] For photopatterning to succeed, the PAG, linear polymer, and bottlebrush polymer should all be soluble in the same solvent for lm casting. Additionally, the approach outlined in this work is easily extended to other chemistries of both the linear and bottlebrush polymers, and other types of reactive groups, enabling control of interfacial properties for a range of applications.

Supporting Information: GPC data for all bottlebrush copolymers; NMR spectra for all bottlebrush copolymers; SAXS data for BB-(PtBA-m-PS)$_1$; FTIR deprotection data for NB-P(tBA-r-S) and BB-(PtBA-m-PS)$_2$.

Acknowledgments The authors thank the National Science Foundation for nancial support under Awards CMMI-1727517 (T.S.L., G.E.S.) and CMMI-1563008 and EEC-144950 (H.M., R.V.). ToF-SIMS analyses were carried out with support provided by the Shared Equipment Authority at Rice University.

References

(1) Ashley, K. M.; Carson Meredith, J.; Amis, E.; Raghavan, D.; Karim, A. Combinatorial investigation of dewetting: polystyrene thin lms on gradient hydrophilic surfaces. Polymer 2003, 44, 769{772, DOI: 10.1016/S0032-3861(02)00779-6.

(2) Karapanagiotis, I.; Evans, D. F.; Gerberich, W. W. Dewetting dynamics of thin polystyrene lms from sputtered silicon and gold surfaces. Colloids and Surfaces A: Physicochemical and Engineering Aspects 2002, 207, 59{67, DOI: 10.1016/S0927-7757(02)00040-7.

(3) Berndt, E.; Behnke, S.; Dannehl, A.; Gajda, A.; Wingender, J.; Ulbricht, M. Functional coatings for anti-biofouling applications by surface segregation of block copolymer additives. Polymer 2010, 51, 5910{5920, DOI: 10.1016/j.polymer.2010.10.002.

(4) Venault, A.; Liu, Y.-H.; Wu, J.-R.; Yang, H.-S.; Chang, Y.; Lai, J.-Y.; Aimar, P. Low-biofouling membranes prepared by liquid-induced phase separation of the PVDF/polystyrene-b-poly (ethylene glycol) methacrylate blend. Journal of Membrane Science 2014, 450, 340{350, DOI: 10.1016/j.memsci.2013.09.004.

(5) Gkaltun, A.; Kang, Y. B. A.; Yarmush, M. L.; Usta, O. B.; Asatekin, A. Simple Surface Modication of Poly(dimethylsiloxane) via Surface Segregating Smart Polymers for Biomicrouidics. Scientic Reports 2019, 9, 7377, DOI: 10.1038/s41598-019-43625-5.

(6) Ordonez, J. S.; Boehler, C.; Schuettler, M.; Stieglitz, T. Silicone rubber and thin-lm polyimide for hybrid neural interfaces A MEMS-based adhesion promotion technique. 2013 6th International IEEE/EMBS Conference on Neural Engineering (NER). 2013; pp 872{875, DOI: 10.1109/NER.2013.6696073.

(7) Boehler, C.; Oberueber, F.; Schlabach, S.; Stieglitz, T.; Asplund, M. Long-Term Stable Adhesion for Conducting Polymers in Biomedical Applications: IrOx and Nanostructured Platinum Solve the Chronic Challenge. ACS Applied Materials & Interfaces 2017, 9, 189{197, DOI: 10.1021/acsami.6b13468.

(8) Seshadri, I.; Silva, A. D.; Meli, L.; Liu, C.-C. C.; Chi, C.; Guo, J.; Truong, H. D.; Schmidt, K.; Arnold, J. C.; Felix, N. M.; Singh, L.; Furukawa, T.; Ayothi, R.; Raley, A.; Farrell, R. A. Ultrathin extreme ultraviolet patterning stack using polymer brush as an adhesion promotion layer. Journal of Micro/Nanolithography, MEMS, and MOEMS 2017, 16, 033506, DOI: 10.1117/1.JMM.16.3.033506.

(9) Nastuta, A.; B. G., R.; Topala, I.; Chiper, A.; Popa, G. Surface modications of polymer

induced by atmospheric DBD plasma in dierent congurations. Journal of Optoelectronics and Advanced Materials 2008, 10, 2038{2042.

(10) Abdou, E. S.; Elkholy, S. S.; Elsabee, M. Z.; Mohamed, E. Improved antimicrobial activity of polypropylene and cotton nonwoven fabrics by surface treatment and modication with chitosan. Journal of Applied Polymer Science 2008, 108, 2290{2296, DOI: 10.1002/app.25937.

(11) Shimizu, K.; Umeda, A.; Blajan, M. Surface Treatment of Polymer Film by Atmospheric Pulsed Microplasma: Study on Gas Humidity Eect for Improving the Hydrophilic Property. Japanese Journal of Applied Physics 2011, 50, 08KA03, DOI: 10.1143/JJAP.50.08KA03.

(12) Jain, S.; Bates, F. S. On the Origins of Morphological Complexity in Block Copolymer Surfactants. Science 2003, 300, 460{464, DOI: 10.1126/science.1082193.

(13) Plueddemann, E. P. Silane adhesion promoters in coatings. Progress in Organic Coatings 1983, 11, 297{308, DOI: 10.1016/0033-0655(83)80012-0.

(14) Jaehne, E.; Oberoi, S.; Adler, H.-J. P. Ultra thin layers as new concepts for corrosion inhibition and adhesion promotion. Progress in Organic Coatings 2008, 61, 211{223, DOI: 10.1016/j.porgcoat.2007.09.044.

(15) Owen, M. J.; Smith, P. J. Plasma treatment of polydimethylsiloxane. Journal of Adhesion Science and Technology 1994, 8, 1063{1075, DOI: 10.1163/156856194X00942.

(16) Walton, D. G.; Mayes, A. M. Entropically driven segregation in blends of branched and linear polymers. Physical Review E 1996, 54, 2811{2815, DOI: 10.1103/PhysRevE.54.2811.

(17) Walton, D. G.; Soo, P. P.; Mayes, A. M.; Soa Allgor, S. J.; Fujii, J. T.; Grith, L. G.; Ankner, J. F.; Kaiser, H.; Johansson, J.; Smith, G. D.; Barker, J. G.; Satija, S. K.

Creation of Stable Poly(ethylene oxide) Surfaces on Poly(methyl methacrylate) Using Blends of Branched and Linear Polymers. Macromolecules 1997, 30, 6947{6956, DOI: 10.1021/ma970698+.

(18) Kim, S.; Yoo, M.; Baettig, J.; Kang, E.-H.; Koo, J.; Choe, Y.; Choi, T.-L.; Khan, A.; Son, J. G.; Bang, J. Perpendicularly Oriented Block Copolymer Thin Films Induced by Neutral Star Copolymer Nanoparticles. ACS Macro Letters 2015, 4, 133{137, DOI: 10.1021/mz500761h.

(19) Kim, K. H.; Kim, M.; Moon, J.; Huh, J.; Bang, J. Bottlebrush Copolymer as Surface Neutralizer for Vertical Alignment of Block Copolymer Nanodomains in Thin Films. ACS Macro Letters 2021, 10, 346{353, DOI: 10.1021/acsmacrolett.0c00879, Publisher: American Chemical Society.

(20) Miyagi, K.; Mei, H.; Terlier, T.; Stein, G. E.; Verduzco, R. Analysis of Surface Segregation of Bottlebrush Polymer Additives in Thin Film Blends with Attractive Intermolecular Interactions. Macromolecules 2020, 53, 6720{6730, DOI: 10.1021/acs.macromol.0c00744.

(21) Mah, A. H.; Laws, T.; Li, W.; Mei, H.; Brown, C. C.; Ievlev, A.; Kumar, R.; Verduzco, R.; Stein, G. E. Entropic and Enthalpic Eects in Thin Film Blends of Homopolymers and Bottlebrush Polymers. Macromolecules 2019, 52, 1526{1535, DOI: 10.1021/acs.macromol.8b02242.

(22) Mei, H.; Laws, T. S.; Mahalik, J. P.; Li, J.; Mah, A. H.; Terlier, T.; Bonnesen, P.; Uhrig, D.; Kumar, R.; Stein, G. E.; Verduzco, R. Entropy and Enthalpy Mediated Segregation of Bottlebrush Copolymers to Interfaces. Macromolecules 2019, 52, 8910{8922, DOI: 10.1021/acs.macromol.9b01801.

(23) Wu, D. T.; Fredrickson, G. H. Eect of Architecture in the Surface Segregation of Polymer Blends. Macromolecules 1996, 29, 7919{7930, DOI: 10.1021/ma9602278.

(24) Minnikanti, V. S.; Archer, L. A. Entropic Attraction of Polymers toward Surfaces and Its Relationship to Surface Tension. Macromolecules 2006, 39, 7718{7728, DOI: 10.1021/ma061377d.

(25) Lee, J. S.; Lee, N.-H.; Peri, S.; Foster, M. D.; Majkrzak, C. F.; Hu, R.; Wu, D. T. Surface segregation driven by molecular architecture asymmetry in polymer blends. Physical Review Letters 2014, 113, 225702, DOI: 10.1103/PhysRevLett.113.225702.

(26) Kelly, J. Y.; Albert, J. N. L.; Howarter, J. A.; Kang, S.; Staord, C. M.; Epps, T. H.; Fasolka, M. J. Investigation of Thermally Responsive Block Copolymer Thin Film Morphologies Using Gradients. ACS Applied Materials & Interfaces 2010, 2, 3241{3248, DOI: 10.1021/am100695m.

(27) Wu, T.; Gong, P.; Szleifer, I.; Vlek, P.; ubr, V.; Genzer, J. Behavior of Surface-Anchored Poly(acrylic acid) Brushes with Grafting Density Gradients on Solid Substrates: 1. Experiment. Macromolecules 2007, 40, 8756{8764, DOI: 10.1021/ma0710176.

(28) Kim, S.; Moses, K. J.; Sharma, S.; Bilal, M.; Cohen, Y. Surface characterization data for tethered polyacrylic acid layers synthesized on polysulfone surfaces. Data in Brief 2019, 23, 103747, DOI: 10.1016/j.dib.2019.103747.

(29) Berquier, J.-M.; Arribart, H. Attenuated Total Reection Fourier Transform Infrared Spectroscopy Study of Poly(methyl methacrylate) Adsorption on a Silica Thin Film: Polymer/Surface Interactions. Langmuir 1998, 14, 3716{3719, DOI: 10.1021/la9703961.

(30) Karkar, Z.; Guyomard, D.; Rou, L.; Lestriez, B. A comparative study of polyacrylic acid (PAA) and carboxymethyl cellulose (CMC) binders for Si-based electrodes. Electrochimica Acta 2017, 258, 453{466, DOI: 10.1016/j.electacta.2017.11.082.

(31) Lindner, A.; Lestriez, B.; Mariot, S.; Creton, C.; Maevis, T.; Lhmann, B.; Brummer, R.

Adhesive and Rheological Properties of Lightly Crosslinked Model Acrylic Networks. The Journal of Adhesion 2006, 82, 267{310, DOI: 10.1080/00218460600646594.

(32) Inui, T.; Sato, E.; Matsumoto, A. Pressure-Sensitive Adhesion System Using Acrylate Block Copolymers in Response to Photoirradiation and Postbaking as the Dual External Stimuli for On-Demand Dismantling. ACS Applied Materials & Interfaces 2012, 4, 2124{2132, DOI: 10.1021/am300103c.

(33) Gurney, R. S.; Morse, A.; Siband, E.; Dupin, D.; Armes, S. P.; Keddie, J. L. Mechanical properties of a waterborne pressure-sensitive adhesive with a percolating poly(acrylic acid)-based diblock copolymer network: Eect of pH. Journal of Colloid and Interface Science 2015, 448, 8{16, DOI: 10.1016/j.jcis.2015.01.074.

(34) Karnal, P.; Jha, A.; Wen, H.; Gryska, S.; Barrios, C.; Frechette, J. Contribution of Surface Energy to pH-Dependent Underwater Adhesion of an Acrylic Pressure-Sensitive Adhesive. Langmuir 2019, 35, 5151{5161, DOI: 10.1021/acs.langmuir.9b00120.

(35) Mogami, H.; Mori, H. Enhanced Heat Resistance and Adhesive Strength of StyreneAcrylic Triblock Copolymer Elastomers by Incorporating Acrylic Acid. ACS Omega 2020, 5, 3678{3688, DOI: 10.1021/acsomega.9b04282.

(36) Cheng, J.; Lawson, R. A.; Yeh, W.-M.; Jarnagin, N. D.; Peters, A.; Tolbert, L. M.; Henderson, C. L. Directed self-assembly of poly(styrene)-block-poly(acrylic acid) copolymers for sub-20nm pitch patterning. Alternative Lithographic Technologies IV. 2012; pp 588{595, DOI: 10.1117/12.918073.

(37) Li, Z.; Zhang, K.; Ma, J.; Cheng, C.; Wooley, K. L. Facile syntheses of cylindrical molecular brushes by a sequential RAFT and ROMP grafting-through methodology. Journal of Polymer Science Part A: Polymer Chemistry 2009, 47, 5557{5563, DOI: 10.1002/pola.23626.

(38) Sanford, M. S.; Love, J. A.; Grubbs, R. H. A Versatile Precursor for the Synthesis of New Ruthenium Olen Metathesis Catalysts. Organometallics 2001, 20, 5314{5318, DOI: 10.1021/om010599r.

(39) Perera, G. M.; Pandey, Y. N.; Patil, A. A.; Stein, G. E.; Doxastakis, M. Reaction Kinetics in Acid-Catalyzed Deprotection of Polymer Films. The Journal of Physical Chemistry C 2012, 116, 24706{24716, DOI: 10.1021/jp308997g.

(40) Mok, M. M.; Kim, J.; Wong, C. L. H.; Marrou, S. R.; Woo, D. J.; Dettmer, C. M.; Nguyen, S. T.; Ellison, C. J.; Shull, K. R.; Torkelson, J. M. Glass Transition Breadths and Composition Proles of Weakly, Moderately, and Strongly Segregating Gradient Copolymers: Experimental Results and Calculations from Self-Consistent Mean-Field Theory. Macromolecules 2009, 42, 7863{7876, DOI: 10.1021/ma9009802.

(41) Xia, Y.; Olsen, B. D.; Korneld, J. A.; Grubbs, R. H. Ecient Synthesis of Narrowly Dispersed Brush Copolymers and Study of Their Assemblies: The Importance of Side Chain Arrangement. Journal of the American Chemical Society 2009, 131, 18525{ 18532, DOI: 10.1021/ja908379q.

(42) Levi, A. E.; Lequieu, J.; Horne, J. D.; Bates, M. W.; Ren, J. M.; Delaney, K. T.; Fredrickson, G. H.; Bates, C. M. Miktoarm Stars via Grafting-Through Copolymerization: Self-Assembly and the Star-to-Bottlebrush Transition. Macromolecules 2019, 52, 1794{1802, DOI: 10.1021/acs.macromol.8b02321.

(43) Wallra, G.; Hutchinson, J.; Hinsberg, W.; Houle, F.; Seidel, P. Kinetics of thermal and acid-catalyzed deprotection in deep-UV resist materials. Microelectronic Engineering 1995, 27, 397{400, DOI: 10.1016/0167-9317(94)00132-E.

(44) La, Y.-H.; Edwards, E. W.; Park, S.-M.; Nealey, P. F. Directed Assembly of Cylinder-Forming Block Copolymer Films and Thermochemically Induced Cylinder to Sphere

Transition: A Hierarchical Route to Linear Arrays of Nanodots. Nano Letters 2005, 5, 1379{1384, DOI: 10.1021/nl0506913.

(45) Kopf, A. H.; Koorengevel, M. C.; van Walree, C. A.; Daorn, T. R.; Killian, J. A. A simple and convenient method for the hydrolysis of styrene-maleic anhydride copolymers to styrene-maleic acid copolymers. Chemistry and Physics of Lipids 2019, 218, 85{90, DOI: 10.1016/j.chemphyslip.2018.11.011.

(46) Jenkins, A. T. A.; Hu, J.; Wang, Y. Z.; Schiller, S.; Foerch, R.; Knoll, W. Pulsed Plasma Deposited Maleic Anhydride Thin Films as Supports for Lipid Bilayers. Langmuir 2000, 16, 6381{6384, DOI: 10.1021/la991649o, Publisher: American Chemical Society.

(47) Tan, T. L.; Kudryashov, V. A.; Tan, B. L. FT-IR Study of a Chemically Amplied Resist for X-ray Lithography. Applied Spectroscopy 2003, 57, 842{849, DOI: 10.1366/000370203322102942.

(48) Patil, A. A.; Pandey, Y. N.; Doxastakis, M.; Stein, G. E. Characterizing acid diusion lengths in chemically amplied resists from measurements of deprotection kinetics. Journal of Micro/Nanolithography, MEMS, and MOEMS 2014, 13, 043017, DOI: 10.1117/1.JMM.13.4.043017.

(49) Ito, H. Solid-state thermolysis of poly(p-t-butoxycarbonyloxystyrene) catalyzed by polymeric phenol: Eect of phase separation. Journal of Polymer Science Part A: Polymer Chemistry 1986, 24, 2971{2980, DOI: 10.1002/pola.1986.080241124.

(50) Wallra, G. Thermal and acid-catalyzed deprotection kinetics in candidate deep ultraviolet resist materials. Journal of Vacuum Science & Technology B: Microelectronics and Nanometer Structures 1994, 12, 3857, DOI: 10.1116/1.587454.

(51) Yadav, V.; Harkin, A. V.; Robertson, M. L.; Conrad, J. C. Hysteretic memory in pH-

response of water contact angle on poly(acrylic acid) brushes. Soft Matter 2016, 12, 3589{3599, DOI: 10.1039/C5SM03134F.

(52) Hu, K.; Bard, A. J. Use of Atomic Force Microscopy for the Study of Surface AcidBase Properties of Carboxylic Acid-Terminated Self-Assembled Monolayers. Langmuir 1997, 13, 5114{5119, DOI: 10.1021/la9700782.

(53) Godnez, L. A.; Castro, R.; Kaifer, A. E. Adsorption of Viologen-Based Polyelectrolytes on Carboxylate-Terminated Self-Assembled Monolayers. Langmuir 1996, 12, 5087{ 5092, DOI: 10.1021/la960485y.

(54) Fears, K. P.; Creager, S. E.; Latour, R. A. Determination of the Surface pK of Carboxylic- and Amine-Terminated Alkanethiols Using Surface Plasmon Resonance Spectroscopy. Langmuir 2008, 24, 837{843, DOI: 10.1021/la701760s.

(55) Uhlmann, P.; Skorupa, S.; Werner, C.; Grundke, K. Characterization of Maleic Acid/Anhydride Copolymer Films by Low-Rate Dynamic LiquidFluid Contact Angle Measurements Using Axisymmetric Drop Shape Analysis. Langmuir 2005, 21, 6302{ 6307, DOI: 10.1021/la046871u.

(56) Wu, S. Surface and interfacial tensions of polymer melts. II. Poly(methyl methacrylate), poly(n-butyl methacrylate), and polystyrene. The Journal of Physical Chemistry 1970, 74, 632{638, DOI: 10.1021/j100698a026.

(57) Pan, F.; Wang, P.; Lee, K.; Wu, A.; Turro, N. J.; Koberstein, J. T. Photochemical Modication and Patterning of Polymer Surfaces by Surface Adsorption of Photoactive Block Copolymers. Langmuir 2005, 21, 3605{3612, DOI: 10.1021/la0477439.

(58) Towle, E. G.; Ding, I.; Peterson, A. M. Impact of molecular weight on polyelectrolyte multilayer assembly and surface properties. Journal of Colloid and Interface Science 2020, 570, 135{142, DOI: 10.1016/j.jcis.2020.02.114.

(59) Vial, J.; Carr, A. Calculation of Hamaker constant and surface energy of polymers by a simple group contribution method. International Journal of Adhesion and Adhesives 1991, 11, 140{143, DOI: 10.1016/0143-7496(91)90013-8.

(60) Stein, G. E.; Laws, T. S.; Verduzco, R. Tailoring the Attraction of Polymers toward Surfaces. Macromolecules 2019, 52, 4787{4802, DOI: 10.1021/acs.macromol.9b00492.

(61) Escal, P.; Save, M.; Lapp, A.; Rubatat, L.; Billon, L. Hierarchical structures based on self-assembled diblock copolymers within honeycomb micro-structured porous lms. Soft Matter 2010, 6, 3202{3210, DOI: 10.1039/C0SM00029A.

(62) Pesek, S. L.; Lin, Y.-H.; Mah, H. Z.; Kasper, W.; Chen, B.; Rohde, B. J.; Robertson, M. L.; Stein, G. E.; Verduzco, R. Synthesis of bottlebrush copolymers based on poly(dimethylsiloxane) for surface active additives. Polymer 2016, 98, 495{504, DOI: 10.1016/j.polymer.2016.01.057.

(63) Yu, D. M.; Smith, D. M.; Kim, H.; Rzayev, J.; Russell, T. P. Two-Step Chemical Transformation of Polystyrene-block-poly(solketal acrylate) Copolymers for Increasing . Macromolecules 2019, 52, 6458{6466, DOI: 10.1021/acs.macromol.9b01323.

(64) Kraton FG Polymers. https://kraton.com/products/Kraton_FG.php, Date Accessed: 04.19.2023.

(65) Ito, H. Microlithography/Molecular Imprinting; Advances in Polymer Science; Springer: Berlin, Heidelberg, 2005; pp 37{245, DOI: 10.1007/b97574.

Graphical TOC Entry